Mater Struct (2024) 57:9
https://doi.org/10.1617/s11527-023-02280-z

ORIGINAL ARTICLE

Improving the pozzolanic reactivity of clay, marl and obsidian through mechanochemical or thermal activation

Vahiddin Alperen Baki · Xinyuan Ke · Andrew Heath · Juliana Calabria-Holley · Cemalettin Terzi

Received: 28 August 2023 / Accepted: 27 November 2023 / Published online: 26 December 2023

Abstract This research investigated the physicochemical properties and pozzolanic reactivity of mechanochemically and thermally treated clay, marl, and obsidian as supplementary cementitious materials (SCMs). The results suggest that the mechanochemical treatment of clay and marl resulted in delamination, dehydroxylation, and amorphisation of the mineral components (including calcite); while for obsidian, the main effect was particle size reduction. Among all samples prepared, the mechanochemically treated obsidian exhibited the best performance as a SCM and achieved marginally higher strength performance at 20% cement replacement compared with the CEM I cement mortar (with on SCM). The thermally activated clay and marl exhibited highest pozzolanic reactivity than the mechanochemically treated counterparts owning to the formation of free lime from calcination of calcite. However, the mechanochemically treated clay and marl were still able to achieve over 80% of the strength activity index and performed much better than the untreated materials. These results indicate that mechanochemical treatment can effectively improve the pozzolanic reactivity of clay minerals that contain calcite up to 68% without directly emitting process CO_2 to the environment (calcination of carbonates), which can be an alternative activation route to the high-temperature calcination-treatment method.

Keywords Clay · Marl · Obsidian · Mechanochemical treatment · Blended cement · Pozzolanic activity

1 Introduction

The consumption of concrete, the most widely used construction material, increased tenfold over the last 65 years and is expected to grow in the next couple of decades [1]. Blending cement with supplementary cementitious materials (SCMs) is one of the most effective methods for reducing the environmental impacts of the concrete industry [2]. Although industrial by-products such as fly ash and GGBFS (ground granulated blast furnace slag) show excellent properties as SCMs, their availability is predicted to decline over the next decades [2]. Clays are one of the most abundant materials in the Earth's crust [3]. Warr [4] indicated that the brittle crust contains around 21.5 wt.% of clay minerals, consists of 7.7 wt.% little or non-expandable 2:1 clay mineral (i.e., illite),

Supplementary Information The online version contains supplementary material available at https://doi.org/10.1617/s11527-023-02280-z.

V. A. Baki · X. Ke (✉) · A. Heath · J. Calabria-Holley
Department of Architecture and Civil Engineering, University of Bath, Bath, UK
e-mail: x.ke@bath.ac.uk

C. Terzi
Department of Civil Engineering, Recep Tayyip Erdogan University, Rize, Turkey

5.7 wt.% 1:1 kaolinite-serpentine minerals, 3.0 wt.% highly expandable 2:1 smectites, and 5.1 wt.% 2:1:1 chlorites. Non-clay materials, such as calcite, quartz, feldspar, and sulfides, were also reported as typical impure phases in mixed clay structures [5]. Marl, which is one of the sedimentary rocks formed by the fragmentation, transportation, accumulation, and sedimentation of the previously formed rocks, constitutes a transition between clay sediments and carbonate sediments [6]. Marl is a soft, loose, and earthy material containing varying amounts of calcium carbonate (35–65% $CaCO_3$), clay, and silt [7].

The research investigating the use of clay and marl as SCMs is limited. The existing research suggested that the calcined marl can replace the cement clinker by 20–65 wt% while achieving desirable 28 days compressive strength performances [8, 9]. The calcium oxide formed as the results of calcite decomposition was the main attribute to the improved strength performances and promoted the formation of calcium silicate hydrate during hydration [9]. As for calcareous clays, the mortars containing 20% calcined calcareous clay result in 10% strength increase after 28 days compared with the reference [10]. At optimum calcination temperature, the presence of calcite in clay structures showed higher pozzolanic activity than their counterpart without calcite due to the formation of glass phase after calcination and synergitic effect between calcite and metastable clay minerals [11]. However, the calcination of carbonate-rich clays is likely to release CO_2 from the heating energy and chemical decomposition, limiting its potential as a low CO_2 SCM. In addition to CO_2 from carbonate decomposition, air pollutants such as NO_x and SO_x can be released during heat treatment [12]. Moreover, some clay minerals might require a high optimum calcination temperature, which might increase the generation of air pollutants [13].

The natural glasses are also quite abundant in the world [14]. Obsidian, known as volcanic glass, was formed due to the sudden cooling of viscous and silicon-rich acidic magma with high water content, consisting of an amorphous siliceous structure with a small crystalline phase [15]. Obsidian can be used as a pozzolan due to high amorphous silica and alumina contents [15]. Their utilisation as SCMs is quite limited in the literature. The sample blended with 25% obsidian showed higher pozzolanic reactivity than fly ash and similar pozzolanic reactivity with blast furnace slag after 90 days of hydration reported by Ustabas and Kaya [15].

Mechanochemical treatment has recently received increased interest as an alternative route to enhance the pozzolanic reactivity of materials rich in aluminosilicates, such as titanium magnetite, fly ash, blast furnace slag, volcanic ash, kaolinite, montmorillonite and muscovite materials, by generating extended crystal defects, new surfaces, and lattice distortion in a short time [12, 16, 17]. With increased activation time, the mechanochemical treatment results in particle comminution and increasing specific surface area up to a maximum fineness, after which further grinding can lead to a decreased specific surface area [18–23]. In addition, amorphization and more adsorbed water were reported after mechanochemical treatment [16, 21, 24]. Although recent advances have improved further understanding of the impact of mechanochemical treatment on a broad range of materials [16, 21, 23, 25, 26], the impact of mechanochemical treatment on natural or mixed mineral deposits has not yet been investigated in detail.

This study investigated the effects of mechanochemical treatment on the physiochemical and pozzolanic reactivity of naturally occurring clay, marl, and obsidian materials. The performances of mechanochemically treated clay, marl, and obsidian as SCMs were compared with non-treated and thermally treated equivalents.

2 Materials and experimental methods

2.1 Materials

The clay and marl used in this study were collected from the Trabzon-Zigana region and obsidian crops from Ikizdere-Rize, Turkey. CEM I 42.5 R type Ordinary Portland cement (5.1% $CaCO_3$) was used for preparing the blended cement paste and mortar. The XRF technique with the fused bead method was used to determine the chemical composition given in Table 1. The loss on ignition (LOI) was determined by heating materials for two hours at 1050 °C.

Table 1 Chemical composition (%) of clay, marl and obsidian determined by X-ray fluorescence analysis. LOI refers to loss on ignition at 1050 °C

Materials	Cement	Clay	Marl	Obsidian
SiO_2	20.1	33.8	18.2	73.3
Al_2O_3	5.4	12.5	7.2	15.6
Fe_2O_3	3.0	5.8	1.6	1.4
CaO	62.8	21.4	37.9	1.0
MgO	2.2	2.6	0.9	0.0
SO_3	2.2	–	0.0	0.0
TiO_2	0.2	0.6	0.1	0.1
K_2O	0.9	1.6	0.7	4.8
Na_2O	0.1	0.5	0.2	3.6
LOI	3.4	22.0	34.2	0.5
Na_2O_{eq}	0.7	1.5	0.6	6.8

$Na_2O_{eq} = Na_2O + 0.658K_2O$

2.2 Sample preparation

2.2.1 Mechanochemical and thermal treatments

The clay, marl, and obsidian were collected as bulk samples from natural deposits and crushed into approximately 0.5–1.0 mm pieces. All materials were put in the drying oven at 105 °C overnight before milling. A standard rotary ball mill was used for making the standard milled materials in powder form at 80 rpm for one hour. Next, mechanochemical treatment of the powder of each mineral was performed in the Retsch PM 100 planetary ball mill with a 250 ml zirconium jar. Fifty zirconium milling balls (10 mm diameter), as recommended by the Retsch PM100 manual, were used to produce optimum grinding results. The mass of powders for grinding in the zirconium jar was 15 g, equivalent to a ball-to-mass ratio of 10/1. The milling speed was stabilized at 500 rpm, and 20, 40, 60 and 120 min of mechanochemical treatment was used. The treated materials are labelled: CL-(R/20/40/60/120/T), ML-(R/20/40/60/120/T) and OBS-(R/20/40/60/120/T), where CL refers to clay, ML refers to marl and OBS refers to obsidian; R indicates the raw material (ground in the rotary ball mill but not thermally or mechanochemically treated), the numbers indicate the mechanochemical treatment time (minute), and T refers to thermal treatment.

Three hours of treatment at 800 °C in a standard air atmosphere was used for clay and marl for thermal treatment. The targeted temperature for thermal treatment was determined according to the initial thermogravimetry analysis of the materials (see later). The crucibles were removed from the oven after thermal activation and then were spread on a steel plate at room temperature for natural cooling.

2.2.2 Preparation of pastes and mortars

Paste with water/binder ratio of 0.5 were made to compare the effect of activated SCMs on the hydration using XRD and TG. Table 2 summarizes the paste mix design, where M refers to mortars in the sample ID, while P refers to paste samples. In addition, reference samples with either 100% OPC or 20% standard milled materials blended systems were produced for comparison. To understand the filler effect and the pozzolanic contribution of clays in a blended system, mechanically milled quartz ($D_{50} = 10.4$ µm) was used to replace 20% of cement for comparison (sample M-Q), as seen in Table 2. The paste specimens were mixed by hand and cured in sealed plastic containers at room temperatures (20 ± 2 °C) for 28 days.

The mortar cubes of the blended cement were prepared according to EN 196–1 with one part binder, half part water, and three parts standard sand to follow the mortar's compressive strength development and porosity [27].

2.3 Blended cement hydration

The hydrating cement was analyzed using XRD and TG at 28 days of hydration. The phase assemblages and the TG of blended cement paste were combined to interpret the formation or consumption of the hydrate phase assemblages semi-quantitatively, where the portlandite depletion is mainly correlated with the pozzolanic reaction. The tangent method was used to determine portlandite from TG analysis and raw materials calcite content.

The bound water results from the R^3 test were used to evaluate clay, marl and obsidian's reactivity. The test for mechanical properties was used to determine whether differently treated clay, marl and obsidian materials result in an acceptable level of strength development when replaced with hydraulic cement. The cumulative pore volumes and pore size distributions of the blended cement mortars after

Table 2 Blended systems mix designs for pastes and mortars

Series	Sample ID	CEM I (%)	Type of the treatment	SCMs (%)	Water/Binder Ratio	Sand/Binder Ratio
Pc	P-PC	100	None	0	0.5	0
	M-PC	100	None	0	0.5	3
Quartz	P-Q	80	None	20	0.5	0
	M-Q	80	None	20	0.5	3
Clay	P-CL-R	80	Standard milled	20	0.5	0
	P-CL-60	80	60 min mechanochemical treated	20	0.5	0
	P-CL-T	80	Thermally treated(800 °C)	20	0.5	0
	M-CL-R	80	Standard milled	20	0.5	3
	M-CL-60	80	60 min mechanochemical treated	20	0.5	3
	M-CL-T	80	Thermally treated(800 °C)	20	0.5	3
Marl	P-ML-R	80	Standard milled	20	0.5	0
	P-ML-60	80	60 min mechanochemical treated	20	0.5	0
	P-ML-T	80	Thermally treated(800 °C)	20	0.5	0
	M-ML-R	80	Standard milled	20	0.5	3
	M-ML-60	80	60 min mechanochemical treated	20	0.5	3
	M-ML-T	80	Thermally treated(800 °C)	20	0.5	3
Obsidian	P-OBS-R	80	Standard milled	20	0.5	0
	P-OBS-60	80	60 min mechanochemical treated	20	0.5	0
	M-OBS-R	80	Standard milled	20	0.5	3
	M-OBS-60	80	60 min mechanochemical treated	20	0.5	3

28 days were determined from the MIP results to asses a higher degree of pozzolanic reaction within each mix.

2.4 Test methods

2.4.1 Particle size distribution, surface properties, and SEM

The particle size distribution (PSD) was determined with a Malvern Mastersizer 2000. Clay, marl and obsidian materials before and after treatment were dispersed in distilled water. Five minutes ultrasonication was carried out for all materials before particle size measurement. The surface textural properties of standard milled materials, mechanochemically and thermally treated clay, marl, and obsidian materials were characterized using the N_2 gas sorption at 77 K using the Autosorb-iQ-C from Quantachrome Anton Paar. The specific surface area of the characterized samples was determined using the Brunauer–Emmett–Teller (BET) method. Before the gas sorption test, the standard milled materials, mechanochemically and thermally treated clay materials were degassed at 30 °C for 16 h under vacuum. The microstructural alteration of materials was determined by the scanning electron microscope (SEM). The surface of the samples was coated with 99% pure gold (Au) for 150 s in an argon gas environment in a coating device (Quorum, SC-7620). Then, the surface morphology of the gold-coated samples was studied with SEM using JEOL, JSM 6610 with an acceleration voltage of 15 kV in a vacuum environment.

2.4.2 Spectroscopic analysis (XRD and FTIR)

A Rigaku-SmartLab instrument was used for X-ray diffraction (XRD) with Cu-Kα radiation with a wavelength of 1.5408 Å and a nickel filter. The tests were conducted with a step size of 0.02° and a counting time of 3 s/step, from 5° to 60° 2θ. The FTIR results were attained from the ATR method. The FTIR spectra were obtained using PerkinElmer (Spectrum 100) brand. The 4000 to 600 cm^{-1} range, 4 cm^{-1}

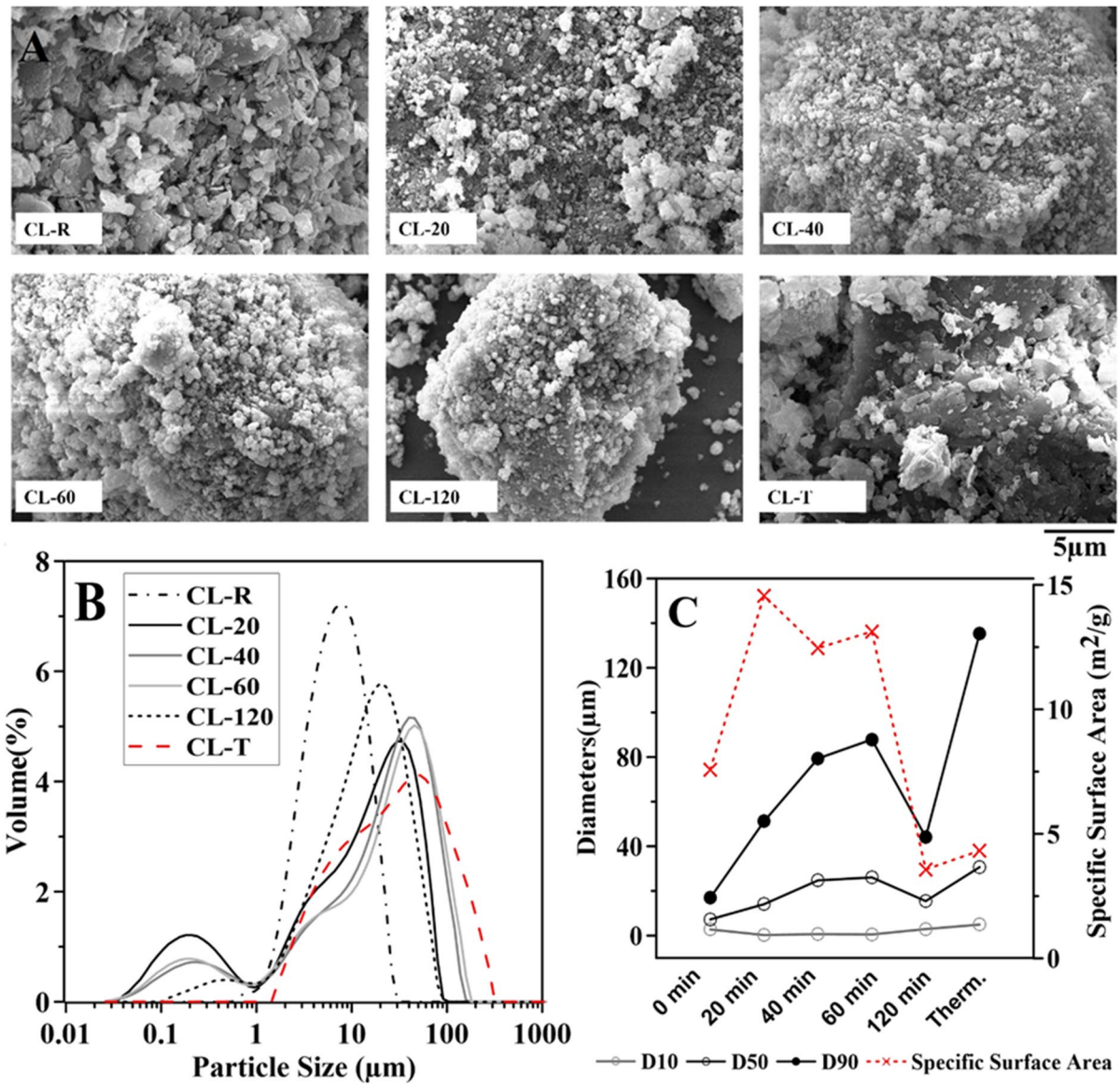

Fig. 1 The **A** SEM images, **B** particle size distributions, and **C** characteristic diameters D_{10}, D_{50}, D_{90} and the BET specific surface area of standard milled, mechanochemically and thermally treated clay

resolution and accumulative 10 scans were used for each measurement.

2.4.3 Thermal analysis

Thermogravimetric measurements of samples in powder form were evaluated using SII Exstar 6000 machine. The samples were heated from 50 to 950 °C with a constant rate of 20 °C/min in an N_2 flow at the flow rate of 20 mL/min.

2.4.4 Mercury Intrusion Porosimetry (MIP)

The MIP measurements were performed using the Thermo Scientific Pascal 440 Series instrument. The external pressure used range from 0.10 to 400 MPa,

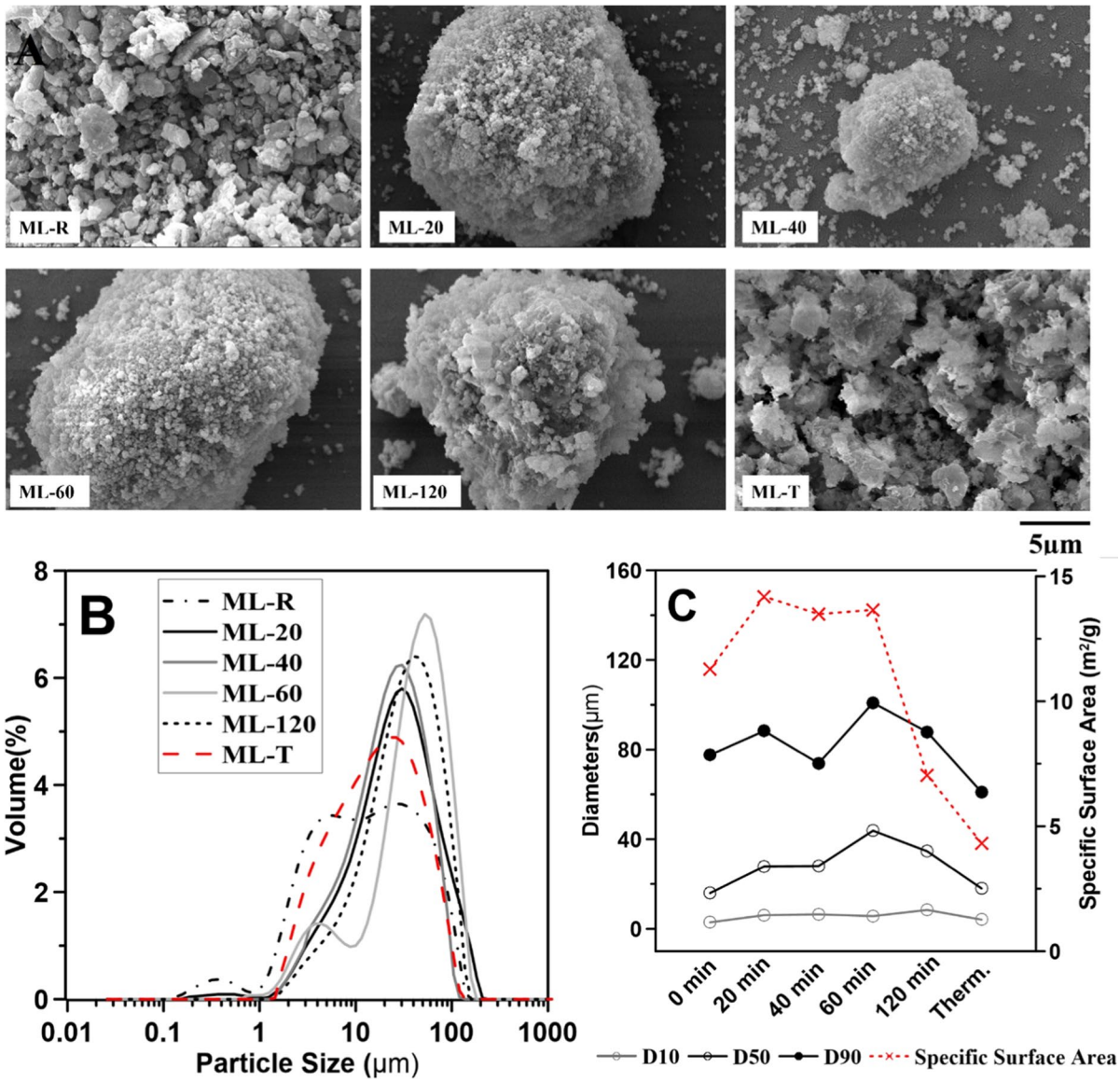

Fig. 2 The **A** SEM images, **B** particle size distributions, and **C** characteristic diameters D_{10}, D_{50}, D_{90} and the BET specific surface area of standard milled, mechanochemically and thermally treated marl

with the mercury contact angle and surface tension of 140° and 0.48 N/m, respectively.

2.4.5 Mechanical properties and R^3 test

Three mortar cubes for each blended mortar were tested for compressive strength using a Utest 6410 instrument at a 6 N/s loading rate after 28 days of curing in a sealed bag at a temperature of (20.0 ± 1) °C.

The SCMs were mixed with portlandite, KOH, K_2SO_4, calcite, and deionized water according to ASTM C1897-20 to form a cement-based environment to determine the bound water capacity of materials. Pastes were cured in sealed containers at 40 °C for seven days. The crushed hydrated pastes were dried in an oven at 105 °C to a constant weight, then heated to 350 °C for 2 h. The chemically bound water content was calculated from the weight difference and used for reactivity evaluation before and after mechanochemical activation.

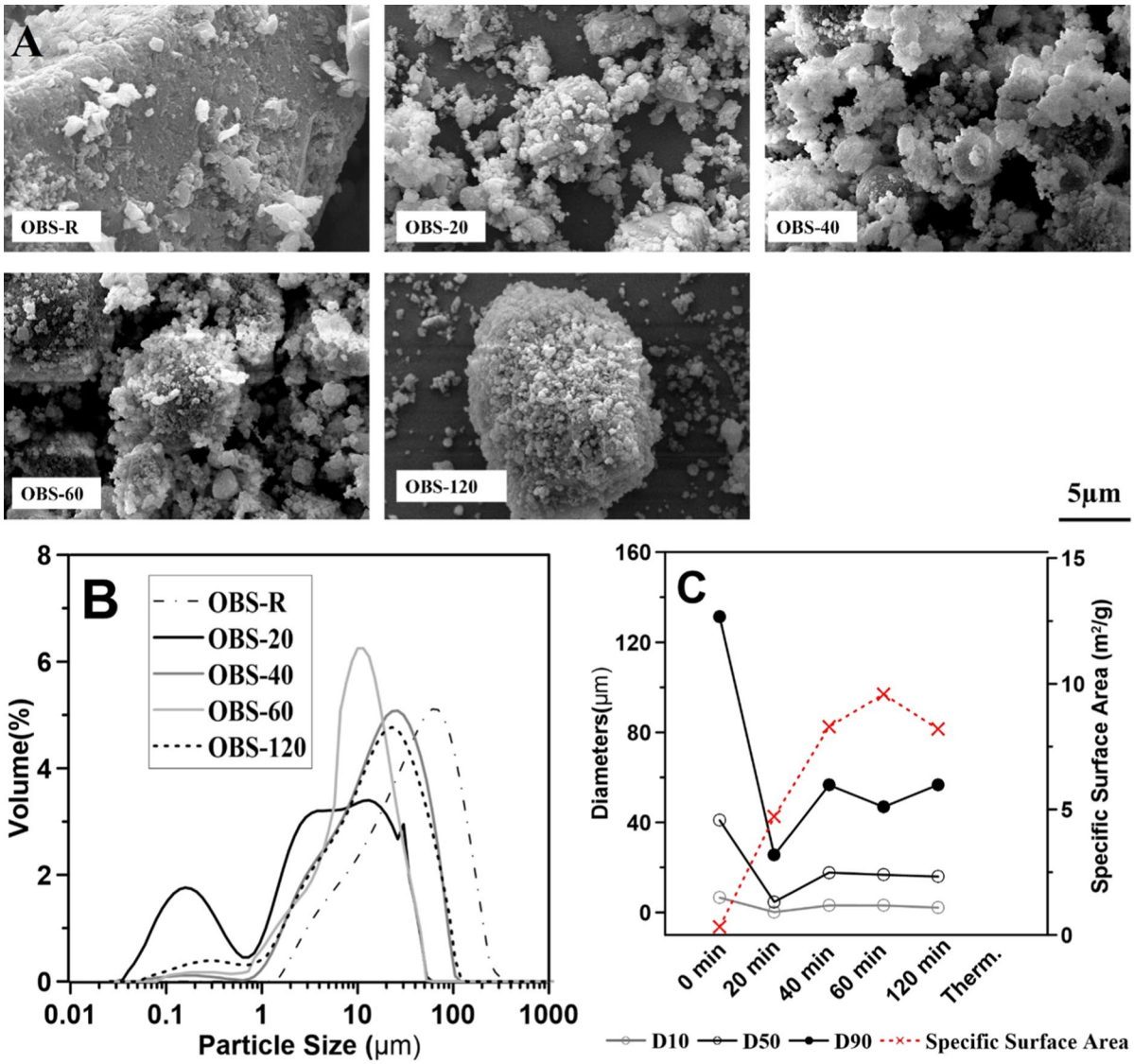

Fig. 3 The **A** SEM images, **B** particle size distributions, and **C** characteristic diameters D_{10}, D_{50}, D_{90} and the BET specific surface area of standard milled, mechanochemically, and thermally treated obsidian

3 Results and discussion

3.1 Mechanochemical and thermal treatment

3.1.1 Particle size distribution and surface texture properties

The natural clay showed polydispersed and irregular shape type morphology (Fig. 1), which did not change with thermal treatment at 800 °C (CL-T) as the morphology of polydispersed and irregular shapes of structures tend to clump with heat treatment [16, 21]. With mechanochemical treatment, the particle size reduction and delamination of the clay layers were observed after 20 min of milling, with the formation of small, rounded particles. Further increase of the milling time to 120 min led to stacked particles and significant agglomeration. A similar morphology alteration was reported by Vdovic et al. [22], where plate-like pseudohexagonal particle structure of kaolinite had become a polydispersed powder with irregular shape particles after 16 min of mechanical

treatment, and increased larger particles with smaller nanoparticles on surfaces was reported after 256 min of milling. Moreover, Dellisanti et al. reported that the irregularly shaped flaky and plate-like particles developed rounded edges and sub-micrometric spherical particles after 20 hours mechanochemical treatment [28].

The raw clay illustrated mono-modal distribution, whereas mechanochemically activated ones showed bi-modal distribution; one mode below 1 μm and one above 1 μm. The clays also retained the mono-modal distribution and showed a higher percentage of the mode above 10 μm after calcination, relative to the raw clay. Both the mechanochemical treatment and the thermal treatment led to a significant shift of the overall particle size distribution to higher values (Fig. 1C). However, after 120 min of milling, the D_{50} values decreased compared with 60 min of milled clay. The specific surface area increased after 20 min mechanical treatment but decreased after 120 min, which can be assigned to significant agglomeration under extended milling [29]. While for thermally activated clay, the specific surface area decreased as the result of sintering and particle agglomeration [30]. It is essential to note that the changes in the specific surface area are not consistent with the particle size measurement. Similar results were also reported by using kaolinite, where the reduction in specific surface area is inconsistent with the particle size [31]. The high specific surface area can be explained not only by the diminution of particle size, but also by the creation of porosity [32]. The inverse relationship between specific surface area and particle size can be related to the porous structure collapse [33]. Additionally, strong agglomeration of particles as a result of intense grinding can decrease nitrogen penetration towards the inside of the agglomerate [34].

The standard milled marl showed angular shape particles (Fig. 2). In contrast, more rounded particles were observed for mechanochemically treated marl, except for 120 min of treatment, which showed a mixture of foil and round shape particles. However, the effect of the milling process is less apparent for marl when compared with clay and obsidian. The standard milled marl showed a bimodal distribution with a D_{50} value of 15.9 μm, which changed to an approximately log-normal distribution after mechanochemical treatment. As the milling time increased to 20 min, mechanochemical treatment slightly increased the median

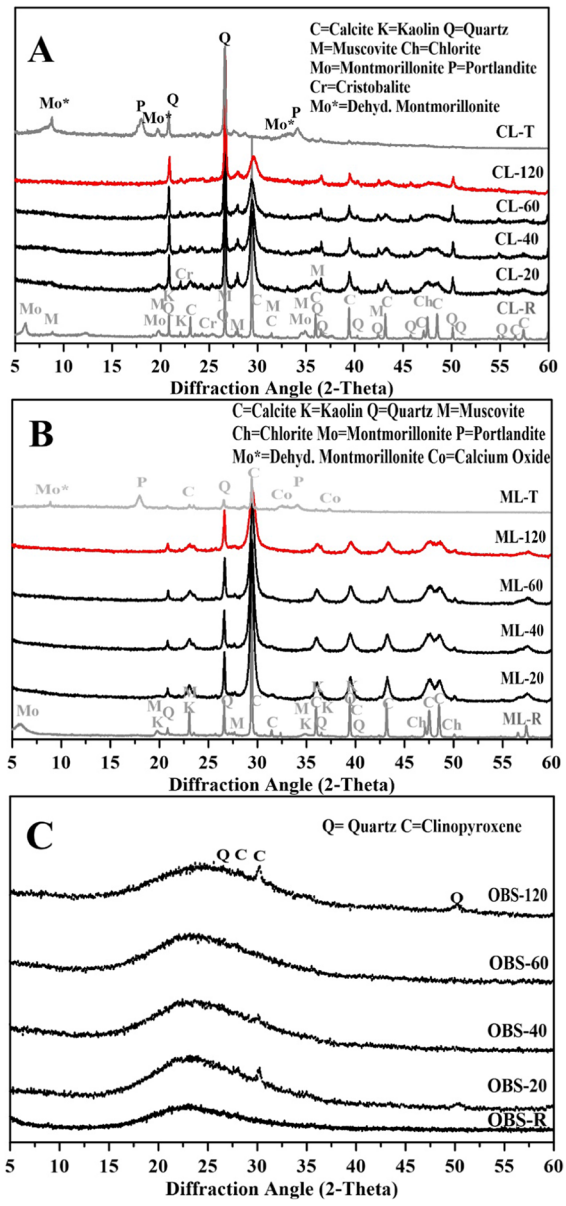

Fig. 4 XRD analysis of original, mechanically and thermally treated clay, marl and obsidian

size of the particles at a 27.9 μm D_{50} values. For prolonged milling times, the particle size distribution generally remained stable. Moreover, a small particle population between 0.1 and 1 μm was not observed for mechanochemically treated marl. This result is consistent with that reported by Hrachova et al., where Ca-saturated minerals are resistant to mechanochemical destruction [19]. A slight increment in

Table 3 PDF card number for XRD analysis

Minerals Name	PDF Number
Kaolinite	#75-0938
Montmorillonite	#13-0135
Chlorite	#73-2376
Muscovite	#06-0263
Calcite	#05-0586
Quartz	#46-1045
Cristobalite	#82-1403
Portlandite	#04-0733
Lime (CaO)	#28-0775
Clinopyroxene	#80-1865

specific surface area was observed after 20 min milling from 11.3 to 14.1 m^2/g. Between 40 and 60 min treatment, the specific surface area did not change significantly. However, 120 min mechanical treatment decreased the specific surface area to 7.0 m^2/g, which can be attributed to the increased agglomeration, similar to that observed for the natural clay. Additionally, thermal activation led to a decrement in the specific surface area in marl, from 11.3 to 4.32 m^2/g, likely due to the sintering and particle agglomeration [30].

The effect of mechanochemical treatment on the obsidian is presented in Fig. 3. Similar to that of clay and marl, mechanochemical treatment impacted on both the particle size distribution and morphology of obsidian. The standard milled obsidian particles showed booklet and angular shape with the D_{50} values around 40.9 µm. The particle morphology was altered after 20 min of mechanochemical treatment, with the D_{50} values significantly decreasing to 4.7 µm. As the milling time increased, the particles lost their angular shape, and very fine and rounded particles due to agglomeration were observed. The agglomeration in the stack became more apparent with the increasing milling time from 20 to 120 min. While mechanochemically treated obsidian and clay materials have similar morphological changes, the PSD of the treated materials have different trends. After short milling (20 min), the size reduction was more apparent than with the clay, but longer treatment did not change the particle size of obsidian materials significantly. It is important to note that the non-treated obsidian shows a mono-modal particle distribution range between 1.5 and 300 µm. However, bi-modal particle size distribution formation becomes apparent for mechanochemical treatment within the 0.02–1 and 1–100 µm. As shown in Fig. 3C, the specific surface area of obsidian gradually increased with prolonged milling time from 0.3 to 9.6 m^2/g after 60 min. At 120 min of milling time, the specific surface area slightly decreased to 8.2 m^2/g.

The main difference between standard milled marl and its standard milled clay and obsidian counterpart was the presence bi-modal particle size distribution, which can be corroborated with the shielding effects during grinding due to the multi-component nature of marl. Different mineral components, such as quartz, calcite, and kaolin requires different milling time to reach the same fineness [35]. Similar results were reported by Perez et al., where the increment of the major fine population ($d < 7$ µm) were observed for the inter-grinding of LC3 cement blends containing higher calcite and less calcined clay [36]. It is also important to note that size reduction, delamination and agglomeration of particles are controlled by the particle size of starting materials and the high-impact ball mill configuration [29, 37], which can explain the difference between the distribution of clay, marl and obsidian after treatment.

3.1.2 Evolution of chemical structures

Figure 4 illustrates the XRD patterns of clay, marl and obsidian after and before different treatment. XRD results show that standard milled clay has clay minerals (kaolinite-montmorillonite-chlorite-muscovite), calcite, quartz, and cristobalite minerals in their structures given in Fig. 4A. Their PDF card numbers are also provided in Table 3.

The breakdown of kaolinite, montmorillonite, muscovite and chlorite peaks was observed after 20 min mechanochemical treatment of clay and marl, which can be assigned to the reduced mineral crystalline size and the amorphization of clay minerals [21], both cristobalite and quartz peaks, on the other hand, remained unchanged. These results are consistent with the studies reported in the literature, where peaks of kaolinite, montmorillonite and muscovite broaden and lower with dry grinding. However, the quartz peak remains unchanged as there is no crystal alteration [19–21, 23, 29, 38]. As for calcite peaks in both clay and marl, the intensity of calcite peaks broadens and lowers with mechanochemical treatment

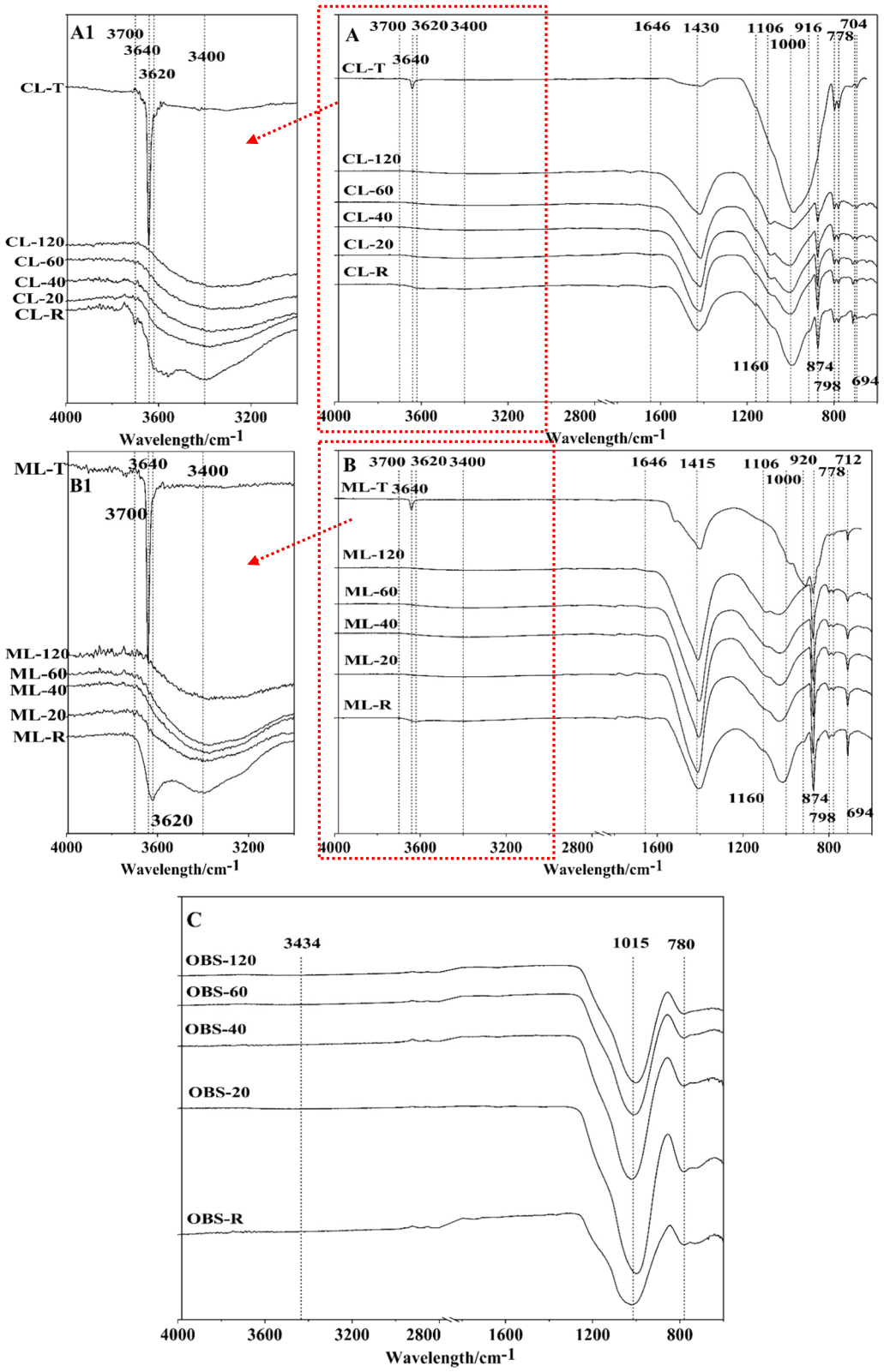
A1
3700
3640
3620
3400
CL-T
CL-120
CL-60
CL-40
CL-20
CL-R
4000
3600
3200
Wavelength/cm-1
A
3700 3620 3400
1646 1430
1106 916 704
1000 778
3640
1160
874
798 694
2800
1600
1200
800
B1
ML-T
ML-120
ML-60
ML-40
ML-20
ML-R
B
1646 1415
1106 920 712
1000 778
1160
874
798 694
C
3434
1015 780
OBS-120
OBS-60
OBS-40
OBS-20
OBS-R

◂**Fig. 5** FTIR spectra of the standard milled, mechanically and thermally treated **A** Clay, **B** Marl and **C** Obsidian

after 20 min of mechanochemical treatment. Beyond 20 min of treatment, the crystalline degree of calcite tended to decrease but was not destroyed wholly after 120 min of milling. This decreasing tendency can be related to the distortion of calcite particles [43] rather than a result of bound CO_2 being released, as is the case with thermal treatment of calcite. Similar results were reported by Chen et al. [44] where the reduction in the intensity of diffraction peaks of calcite can be corroborated with the structural distortion and grain size decreases. The limitation for decreasing the crystal structure of calcite can be attributed to the aggregation of fine particles, which tend to stop further particle size alteration [43]. Similar results were found by Li et al. [43] who reported that the calcite peak intensity decreases in the early stages of mechanical treatment. During the middle grinding stage, calcite peaks did not show a further reduction in intensity due to aggregation, which hindered the breakage of particles [43].

For thermal treatment, the peak intensity of clay minerals (except for muscovite) decreases with calcination in both clay and marl, which can be assigned to altering inert clay structure to the amorphous phase by removing their structural hydroxyl ions [39]. The absence of montmorillonite peak at about 6° (2θ) and broad peak at 9° (2θ) after thermal activation (in both clay and marl) can be attributed to the dehydrated structure of montmorillonite to a 10 Å TOT structure [40, 45]. Previous research has also shown that muscovite and quartz structures are unchanged with thermal treatment up to 800 °C [41]. The presence of portlandite can be attributed to the formation of very reactive lime (CaO) during calcination, which has slaked during storage [42].

For obsidian, the presence of quartz and clinopyroxene was observed in Fig. 4C, but both sets of peaks were small compared to the amorphous hump in the XRD spectra. The width of the amorphous hump centred at around 22° (2θ) further increased, and the crystalline phases disappeared after milling for 40 min. A similar trend was observed after mechanochemical treatment of diopside [46]. After a threshold time, mechanical milling transformed crystalline into amorphous materials by distorting their long-range atomic order and accumulating defects [47]. However, the quartz peaks at 26.6° (2θ) and 50.1° (2θ) were observed at the extended grinding time. The initial milling stage can result in the breakdown of covalent bonds of silicate networks to form $Si–O^-$, which causes the formation of silanol groups by taking atmospheric moisture during the late milling stage. Therefore, the appearance of quartz peaks can be related to the silanol groups' partial recrystallization or polycondensation [17].

The changes of chemical bonds in clay, marl and obsidian before and after different treatments were assessed using the FTIR, as summarised in Fig. 5. The typical bands observed for clay and marl materials are: 3700 and 3620 cm^{-1} (OH stretching vibrations); 1106, 794 and 754 cm^{-1} (Si–O–Si stretching and bending vibration); 1020 and 694 cm^{-1} (Si–O vibrations); 916 cm^{-1} (Al–OH); 1160, 798 and 778 cm^{-1} (quartz); 1454, 874 and 704 cm^{-1} (CO_3 vibration); 3400 and 1646 cm^{-1} bending vibration of water [20, 43, 48]. Mechanical treatment flattened the structured O–H stretching bands around 3700 cm^{-1} and inner O–H bonds at 3620 cm^{-1}, which disappeared with increasing grinding time. The intensity reduction of O–H vibration bands can be attributed to the structural collapse of clay minerals, and the formation of amorphous hydrous compounds, as well as the broadening and decreasing of Si–O stretching vibrations at 1000 cm^{-1}, which also confirmed the destruction and distortion of clay minerals structure [20]. The appearance of a SiO stretching vibrations at 1106 cm^{-1} after 120 min grinding can be attributed to the formation of alumina or siloxane surface due to the removal of hydroxyl [39]. The peak sharpness for Al–OH bending vibration at 916 cm^{-1} decreased with mechanical treatment. The quartz peaks at 1160, 798 and 778 cm^{-1} do not change with mechanical treatment, consistent with XRD results given in Fig. 4A and B. Furthermore, the absorption bands of calcite at 1430, 1415, 874, and 704 cm^{-1} gave less sharp peaks with increase in mechanical treatment time due to a reduction in crystal sizes [43]. On the other hand, the thermal treatment resulted in modifying the characteristic bands of clay minerals and carbonates, where the heat treatment led to dehydroxylation of clay minerals with disappearing of the –OH stretching bands at 3700 and 3620 cm^{-1}, similar to that reported by Srasra et al. [49]. Figure 5C shows the structural change of the obsidian minerals after mechanochemical treatment. The typical bands observed for

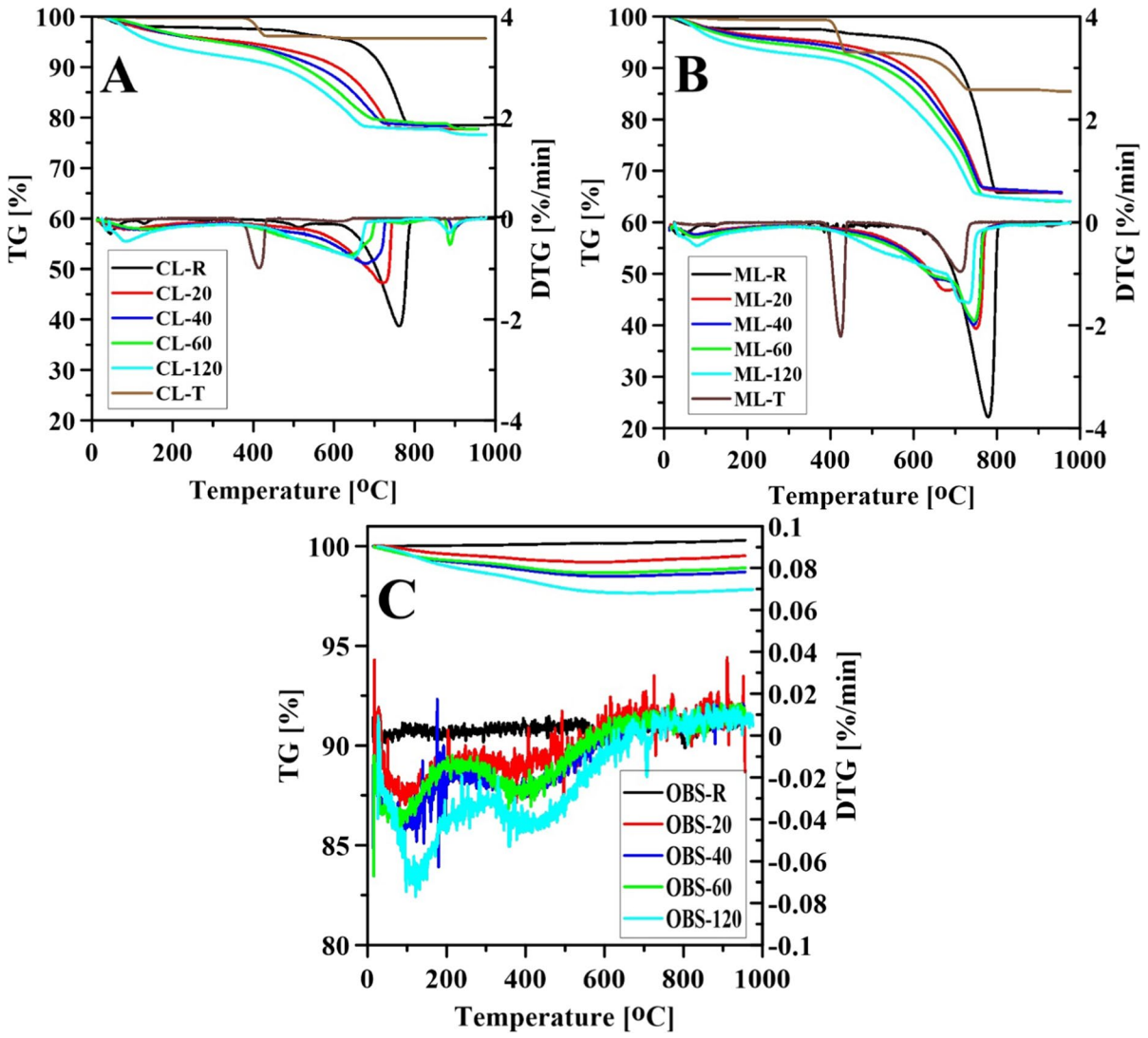

Fig. 6 TGA analysis for standard milled, mechanically and thermally treated **A** clay, **B** marl and **C** obsidian

obsidian are 1000–1200 cm^{-1}(asymmetric stretching Si–O vibrations) and 700–900 cm^{-1}(Si–O–Si bending vibrations and Si–O stretching vibrations in SiO_4 tetrahedra [50]. The increase of mechanochemical treatment time led to slight shift for the Si–O band to lower wavenumber suggesting lower degree of polymerisation.

The TGA analysis of clay, marl and obsidian after different treatment processes is shown in Fig. 6. The TGA pattern of clay and marl indicates similar behaviour because of their similar mineral composition. The first mass loss region from 25 to 180 °C can be related to the loss of adsorbed water [51]. With milling time increase, the weight loss increased by 1.5,1.2, and 2.5% for clay, marl and obsidian, which can be attributed to the absorption of the released hydroxyl group caused by breaking OH bonds during mechanochemical treatment and the adsorption of atmospheric water by a freshly created surface [16, 21]. The presence of impurities and decomposition of organic matter (less than 1%) can be seen from the mass loss between 180 and 450 °C [51]. The standard milled clay and marl showed a dehydroxylation peak centred at 520, 690 and 880 °C for kaolinite,

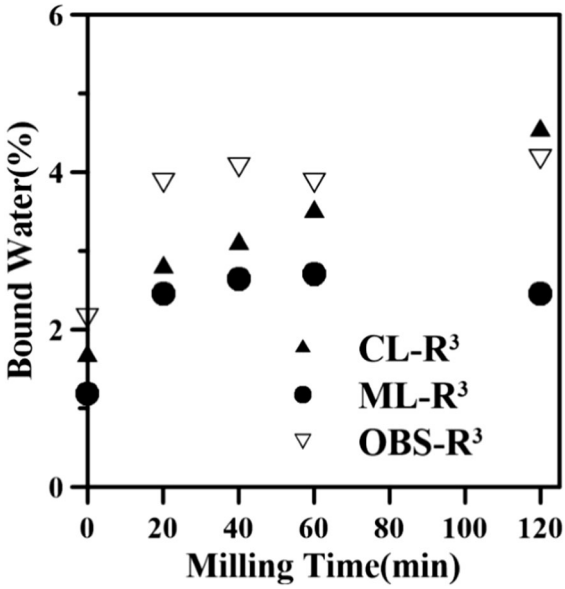

Fig. 7 The bound water test results according to the R^3 test

montmorillonite and muscovite, respectively [16]. However, the obsidian did not show a dehydroxylation peak due to the lack of hydroxyl groups or chemically combined water in their structure. It is also important to note that the decomposition of calcite between 600 and 800 °C can overlap with the presence of kaolinite and montmorillonite [51, 52]. As the milling time increased, the clay and marl main mass loss peak shifted towards lower temperatures with decreasing intensity**.** The main mass loss peak of clay shifted from 762 °C to the lower temperature of 644 °C, while for marl, it dropped from 780 to 720 °C. This suggests that mechanochemical treatment decreased the required dehydroxylation temperature by weakening the OH bond [53]. The dehydroxylation mass loss peak became larger and asymmetric due to the formation of disordered and partially amorphous structures [23]. Similar results were also reported by Aglietti et al. [31] where the temperature of the dehydroxylation peak shifting towards the lower temperature after grinding can be associated with a decrease in the bond energy of the hydroxyl groups. These results also correlated with the XRD results, where amorphization was observed. It is also important to note that compared with marl, the higher main peak shift of clay to a lower temperature can be related with mineral composition, which is likely related to the higher quartz and lowest calcite content. Mako et al [53] reported that increased quartz content showed an acceleration of the mechanically induced amorphization of the kaolinite structure as quartz grains act as grinding bodies.

Additionally, the main peak shift towards lower temperature can be attributed to the lowering decomposition peak of $CaCO_3$ with grinding [54]. In marl, calcite was not completely decomposed after thermal treatment. This corroborates with the XRD and FTIR results, where the decomposition of calcite was only partly observed, similar to the results reported in the literature [10]. For both thermally activated clay and marl, a new TG drop at 400 °C showed portlandite formation, presumably caused by rehydration of calcium oxide after thermal activation. This suggests that it is difficult to isolate at room temperature [52], corroborating with XRD results in Fig. 4.

3.1.3 Bound water test

Figure 7 shows the bound water results for clay, marl and obsidian materials according to the R^3 test. The bound water test was used to predict the reactivity of materials by measuring bound water. The optimal mechanochemical treatment duration for further investigation was chosen from R^3-based pozzolanic reactivity results. A standard milled clay bound 1.6% water, which significantly increases with milling. The bound water content of mechanochemically treated clay increased as the milling time increased from 20 to 120 min. Standard milled marl (zero milling time) had the lowest bound water ratio of 1.1%. The bound water capacity of the mechanochemically treated marl increased as the milling time increased from 0 to 20 min; after which the bound water ratio increased slightly peaking at 60 min. Even though the bound water capacity seems to increase with milling, marl has the lowest water-bound capacity among all the materials, which can be attributed to the greater extent of calcium content, which reduces the efficiency of mechanochemical treatment [19]. Obsidian has a 2.1% bound water capacity, the highest initial bound water ratio. The initial bound water results also are consistent with the compressive strength results, where the obsidian blended system has the highest strength activity index. The bound water capacity nearly doubled after only 20 min of milling. Beyond 20 min, a slight increase in bound water with increased milling time was observed, although there

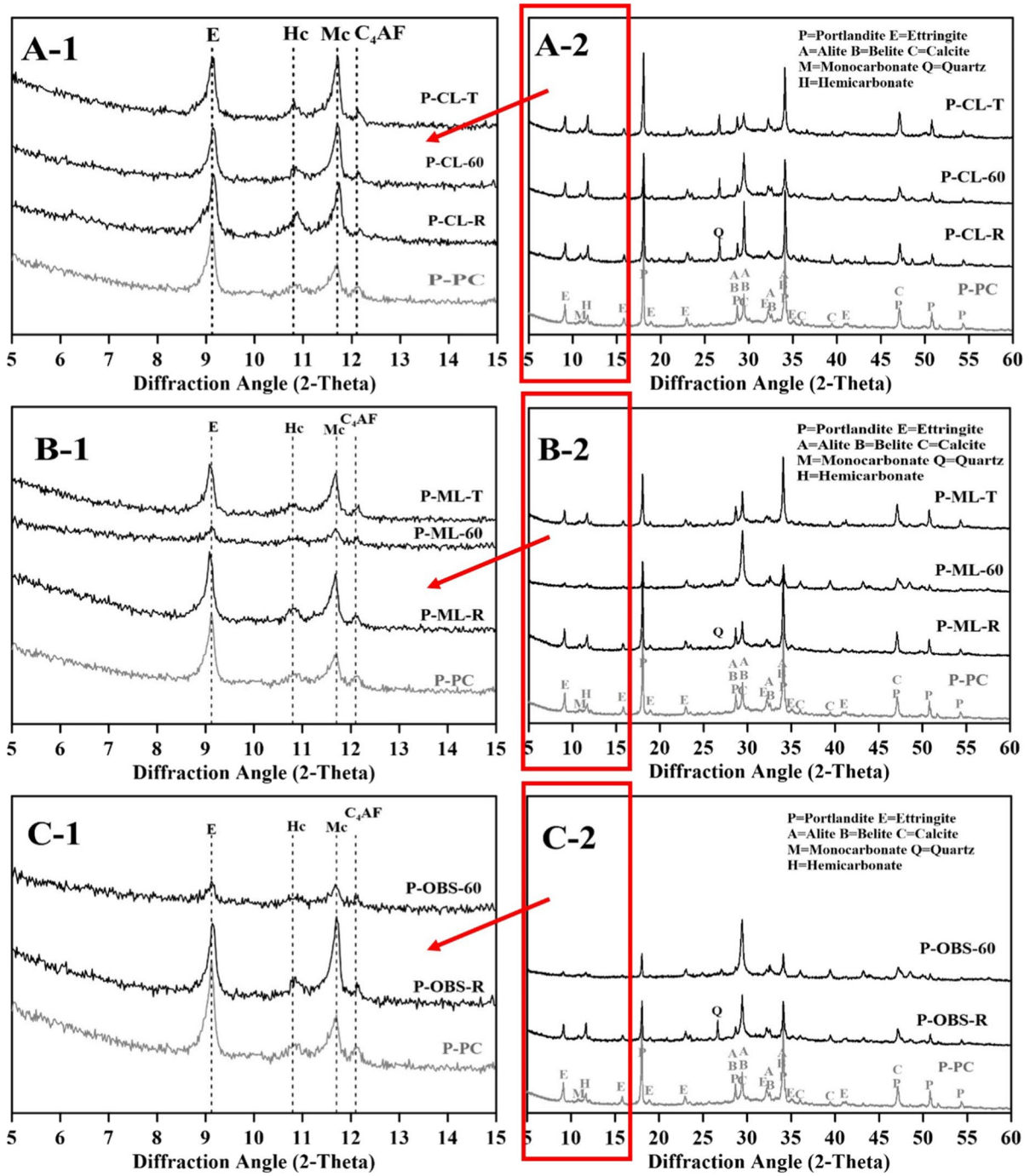

Fig. 8 XRD analysis of reference, standard milled, 60 mechanochemical treated and thermal treated **A** clay, **B** marl and **C** obsidian blended system

is some minor scatter in the data. Similar results were found by Ustabas and Kaya, where the pozzolanic activity index increased with milling time [15].

Based on the results shown in Fig. 7, it is essential to note that the bound water increased with milling for all materials, demonstrating that mechanochemical

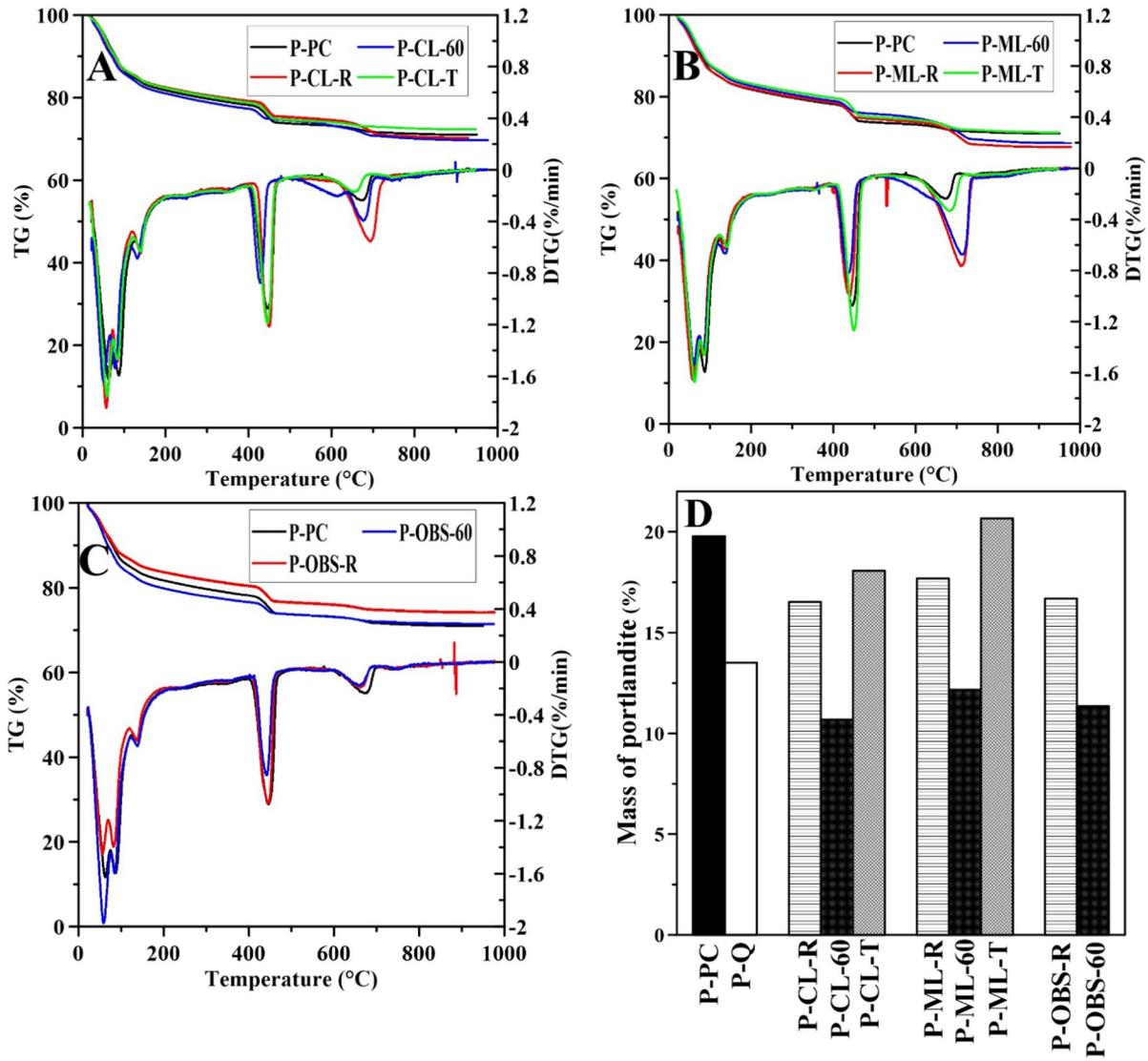

Fig. 9 TGA results of blended cement pastes containing 20% standard milled, 60 min milled and thermally heated **A** clay, **B** marl and **C** obsidian

treatment increased the pozzolanic properties of all three materials. The increasing reactivity was also reported after mechanochemical treatment in the literature [20, 21]. In addition, 60 min mechanochemical treatment was chosen as an optimal treatment time and will be used for comparing the pozzolanic reactivities for the following sections. Combining the bound water results present in this study and the results reported in the literature [55], the bound water content of SCMs used in this study, activated with mechanochemical activation, is similar to highly reactive pozzolans reported in literature, such as siliceous fly ashes (1.25–3.5%), calcareous fly ashes (3.125–5.375%), calcined clays (4.1–15.75%), ground granulated blast furnace slags (3.25–7%), and natural pozzolan (1.875–4.5%).

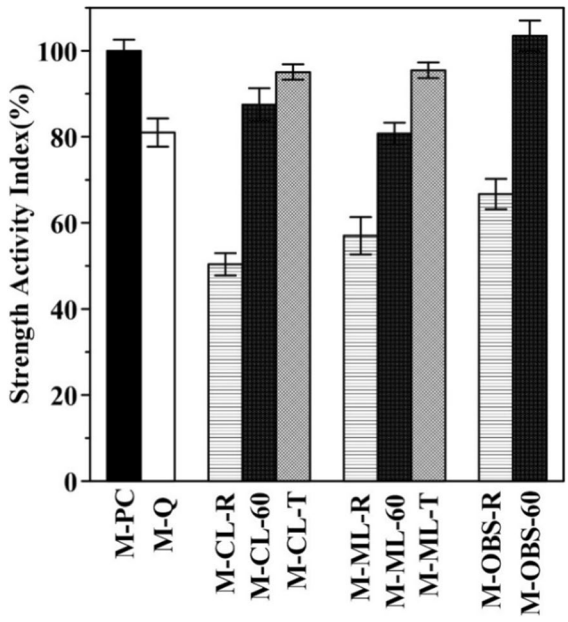

Fig. 10 28 days compressive strength results of reference, standard milled, 60 min mechanochemical treated and thermal treated clay, marl and obsidian blended samples

3.2 Performances as SCMs in cement paste and mortar

3.2.1 Mineralogy of blended cement paste

The consumption and formation of the individual phases were investigated using the XRD and TGA (Figs. 8 and 9). The absolute intensity of XRD doesn't represent the absolution quantity, but the TG data is more representative in terms of comparing quantitative content between different materials. Replacing 20% of the cement clinker with standard milled, mechanochemically, and thermally treated pozzolans did not lead to the formation of new phases in the hydrated blended cement paste. The main differences between different mix designs were changes in the relative content of portlandite, AFt and AFm. The standard milled clay and marl blended system showed negligible changes in the relative intensity of portlandite, AFt and AFm phases, which can be attributed to the low pozzolanic reactivity and dilution effect of standard milled clay and marl. Similar results were observed in the mass percentage of portlandite given in Fig. 9D. It can be observed that negligible portlandite reductions can be attributed to dilution and low pozzolanic reactivity. On the other hand, the portlandite peak intensity substantially decreases with the addition of standard milled obsidian. These results also corroborate the bound water and TGA test results, where obsidian showed the highest bound water and portlandite consumption among standard milled pozzolans. It is also important to note that blended cement samples containing mechanochemically or thermally treated materials led to significant portlandite reduction. The portlandite reduction is mainly attributed to the enhanced reactivity of pozzolans after treatment. TGA results also confirm that the blended system prepared with mechanochemically treated materials showed a significant decrease of portlandite, with around 35% reduction even after considering the dilution effect. In addition, the portlandite consumption is less apparent for thermally treated materials blended systems compared with mechanochemical treatment, even though the XRD data is qualitative only. TGA results showed that the portlandite level increased for the sample incorporating thermally treated clay and marl compared with the blended counterparts of standard milled and mechanochemically treated materials. The formation of portlandite after thermal treatment due to rehydration of CaO during the decomposition of $CaCO_3$ might be a significant reason why thermally treated clay and marl blended system showed a high level of portlandite peaks [56].

The OPC (P-PC) hydration products in this study corroborated with the results commonly reported in the literature. Some hemicarbonate and monocarbonate are formed from the small (5.1%) quantity of carbonate present in the clinker [57]. Generally, relatively higher content of AFm phases and lower content of ettringite were observed for the pozzolan blended system compared to the reference. The increased AFm content can be attributed to the reaction between additional aluminates phases with calcium carbonate to form hemi and monocarbonate [58]. In that case, ettringite does not decompose in reaction with C_3A [58]. On the other hand, the ettringite phase was significantly reduced in samples prepared with mechanochemically treated marl and obsidian. This is likely due to the enhanced reactivity of Al element in the mechanochemically treated clay minerals [16, 21], which lead to

ettringite destabilisation and formation of increased AFm phases [21, 59].

3.2.2 *Mechanical performance and Porosity*

The 28-day strength activity index (SAI) of blended cement was assessed according to the ASTM C618 [60]; it states that the mortar made with 20% substitution must provide at least 75% strength activity index at 28 days. The reference mortar in this study (M-PC), prepared with 100% PC, indicated a 47.9 ± 1.9 MPa compressive strength value. The mortar sample prepared with 20% quartz (M-Q, inert filler), showing filler effect, had an 81% SAI value compared with the reference.

As shown in Fig. 10, the lowest strength activity indexes were observed for mortars incorporating standard milled materials, consistent with the low portlandite consumption value from TGA results in Fig. 9. These results can be related to the low pozzolanic reactivity of standard milled materials. It is also important to note that although standard milled materials showed similar particle size distribution with quartz, the standard milled materials blended system has low strength values compared with M-Q. The higher SAI value of the quartz blended system can be attributed to the quartz particles (1–10 µm) contribution towards the pozzolanic reaction [61]. The 60 min mechanochemical treatment of clay, marl and obsidian can significantly increase strength compared to their standard milled counterparts. The mechanochemical-treated obsidian blended system had the highest strength activity value of 103%. On the other hand, both mechanochemical treated clay and marl blended samples had almost the same strength activity indexes of 88%, well above the acceptable limit in ASTM C618. Additionally, the highest SAI values of mechanochemically treated materials compared to M-Q sample also confirm the improved pozzolanic activity in addition to the filler effect. This increase is explained by the pozzolanic properties of mechanochemically treated materials, which filled more space by reacting with $Ca(OH)_2$ to form secondary C–S–H, as indicated by the XRD results and pore size distribution. A similar strength increment was also reported in the literature [21]. It is important to note that thermally treated clay and marl slightly surpass the strength activity index of its mechanochemically treated ones with 95.06 and 95.48% SAI values, respectively. Similar phenomena were observed in thermally treated clay and marl samples [9, 10]. The higher SAI results of thermally treated clay and marl can be attributed to the formation of amorphous phases, such as aluminates, after thermal treatment [51]. The results shown in this study suggest that mechanochemical treatment can effectively activate carbonate-bearing clay materials. However, the presence of calcite increases the sample resistivity against mechanochemical treatment and results in lower pozzolanic reactivity.

Figure 11 shows cumulative porosity and the pore size distribution of reference, 20% standard milled, mechanochemically and thermally treated clay, marl and obsidian blended mortars after 28 days. For mortar samples incorporating 20% standard milled clay, marl and obsidian, the higher overall intrudable porosity and a higher percentage of both capillary and gel pores were observed compared with the reference mortar sample. These results corroborate with the low strength activity index results of standard milled pozzolan blended system, suggesting high porosity and low compressive strength can be assigned to less hydration product due to low pozzolanic reactivities and dilution effect [41]. The low pozzolanic reactivity of these samples are also noticeable from the major trend of XRD and TGA shown in Figs. 8 and 9, where the standard milled pozzolan blended system showed the lowest portlandite consumption. As for mortars containing 20% mechanochemically treated clay, and marl, a significant reduction of capillary pores and an increase of the gel pore can be observed. The trend is slightly different for mechanochemically treated obsidian blended samples, where pore size refinement is more pronounced than clay and marl-related mortars. The mechanochemical treated blended mortars have lower cumulative porosity compared with the reference, except for 60 min treated clay which depicted higher cumulative porosity than the reference. The highest portlandite consumption from TGA results in Fig. 9 also confirmed why the mechanochemically treated pozzolan blended system pore size is shifted to a lower size range. A similar trend can also be observed for the thermally treated clay and marl blended mortars, where the reduction of capillary pore percentage and increasing gel pores is significant. Both thermally treated clay and marl blended mortars showed similar or lower cumulative porosity than reference mortar.

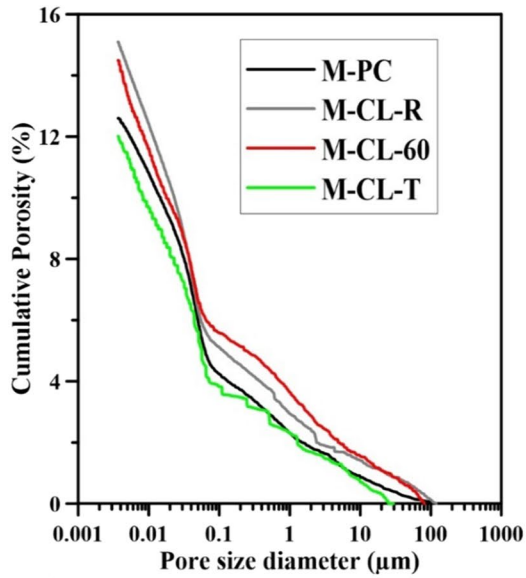
Cumulative Porosity (%)
Pore size diameter (μm)
M-PC
M-CL-R
M-CL-60
M-CL-T

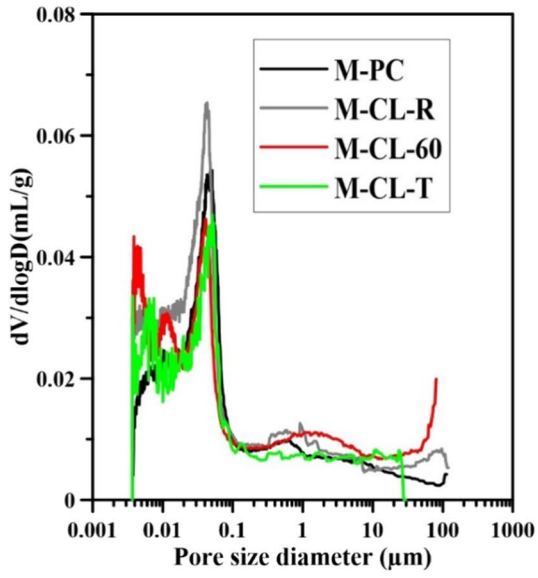
dV/dlogD(mL/g)
Pore size diameter (μm)
M-PC
M-CL-R
M-CL-60
M-CL-T

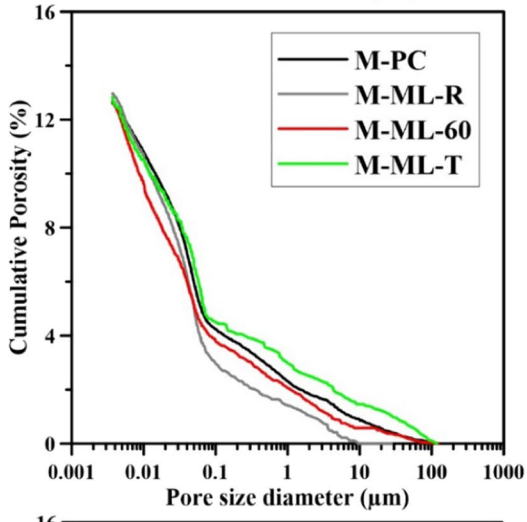
Cumulative Porosity (%)
Pore size diameter (μm)
M-PC
M-ML-R
M-ML-60
M-ML-T

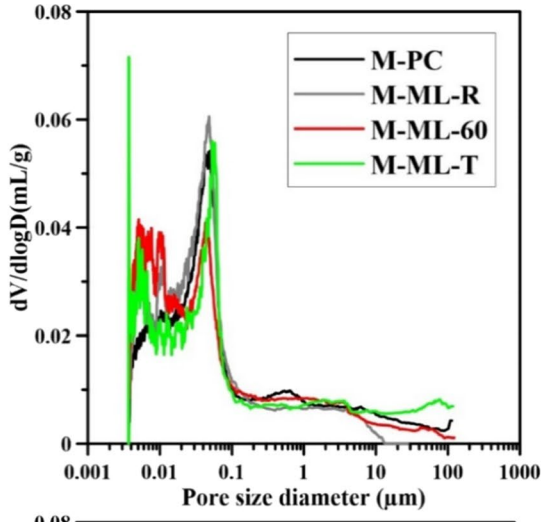
dV/dlogD(mL/g)
Pore size diameter (μm)
M-PC
M-ML-R
M-ML-60
M-ML-T

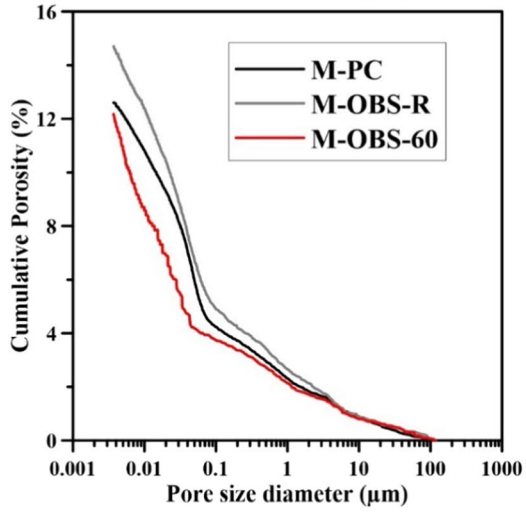
Cumulative Porosity (%)
Pore size diameter (μm)
M-PC
M-OBS-R
M-OBS-60

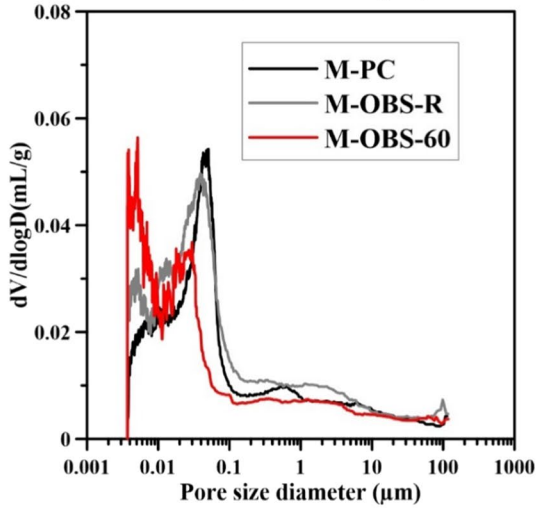
dV/dlogD(mL/g)
Pore size diameter (μm)
M-PC
M-OBS-R
M-OBS-60

◂**Fig. 11** MIP results of reference, standard milled, 60 min mechanochemical treated and thermal treated **A** clay, **B** marl and **C** obsidian blended system

4 Conclusion

This study investigates the physicochemical and pozzolanic properties of clay, marl and obsidian materials treated mechanochemically or thermally. Both treatment methods enhance the pozzolanic reactivity but have different physicochemical, chemical, and structural characteristics. For the clay and marl assessed in this study, the thermal treatment led to an increment in particle size and the specific surface areas due to sintering and agglomeration, while mechanochemical treatment resulted in size reduction, increased surface areas, and delamination after 20 min of activation. The prolonged milling process did not further change the particle size of materials and decreased specific surface area. Mechanochemical activation for 20 min led to a substantial increase in the specific surface area of obsidian, correlated with the decrease in particle size. The specific surface area gradually increased up to 60 min and slightly decreased after 120 min as a consequence of increasing particle agglomeration in the stack, though longer treatment did not change the particle size distribution of obsidian significantly.

In comparison with 100% PC mortars, blended cement mortars prepared with 20% mechanochemically treated clay or marl achieved 88% and 81% strength activity index at 28 days, these values are 37.7% and 24% higher than their standard milled counterparts. The blended cement mortars prepared with thermally treated clay and marl resulted in slightly higher strength than their mechanochemically treated counterparts due to the presence of lime and $Ca(OH)_2$ after the thermal treatment. Mechanochemically activated obsidian powder exhibited the highest pozzolanic activity, which was 37% higher than its standard milled counterpart. This study demonstrated that it is possible to effectively utilise carbonate-bearing materials as supplementary cementitious materials without directly releasing CO_2 into the atmosphere and improve the pozzolanic reactivity of natural pozzolans, such as obsidian.

Acknowledgements VAB acknowledges the Turkish Ministry of National Education for sponsoring his PhD study. The authors would also like to thank Prof Dr Fatih Yilmaz for his help with collecting the TGA and FTIR data and Dr Olivier Camus for his assistance with configurating the MIP and nitrogen sorption testing.

References

1. Habert G et al (2020) Environmental impacts and decarbonization strategies in the cement and concrete industries. Nat Rev Earth Environ 1(11):559–573
2. Juenger MCG, Siddique R (2015) Recent advances in understanding the role of supplementary cementitious materials in concrete. Cem Concr Res 78:71–80
3. Scrivener K et al (2018) Calcined clay limestone cements (LC3). Cem Concr Res 114:49–56
4. Warr LN (2022) Earth's clay mineral inventory and its climate interaction: A quantitative assessment. Earth Sci Rev 234:104198
5. Habert G et al (2009) Clay content of argillites: influence on cement based mortars. Appl Clay Sci 43(3–4):322–330
6. Boggs S (2016) Principles of sedimentology and stratigraphy
7. Gutiérrez De La Cruz LV (2018) Petrology of the sedimentary rocks—J. T. Greensmith 1988
8. Østnor T, Justnes H, Danner T (2015) Reactivity and microstructure of calcined marl as supplementary cementitious material. In: Calcined clays for sustainable concrete. Springer, Dordrecht
9. Rakhimov RZ et al (2017) Properties of Portland cement pastes enriched with addition of calcined marl. J Build Eng 11:30–36
10. Danner T, Norden G, Justnes H (2018) Characterisation of calcined raw clays suitable as supplementary cementitious materials. Appl Clay Sci 162:391–402
11. Danner T, Norden G, Justnes H (2020) The Effect of Calcite in the Raw Clay on the Pozzolanic Activity of Calcined Illite and Smectite. In: Calcined Clays for Sustainable Concrete. Springer, Singapore.
12. Kumar R, Kumar S, Mehrotra SP (2007) Towards sustainable solutions for fly ash through mechanical activation. Resour Conserv Recycl 52(2):157–179
13. Hollanders S et al (2016) Pozzolanic reactivity of pure calcined clays. Appl Clay Sci 132:552–560

14. Varshneya AK (1994) Fundamentals of inorganic glasses. Academic Press, Boston
15. Ustabas I, Kaya A (2018) Comparing the pozzolanic activity properties of obsidian to those of fly ash and blast furnace slag. Constr Build Mater 164:297–307
16. Baki VA et al (2022) The impact of mechanochemical activation on the physicochemical properties and pozzolanic reactivity of kaolinite, muscovite and montmorillonite. Cem Concr Res 162:106962
17. Djobo JNY et al (2016) Mechanical activation of volcanic ash for geopolymer synthesis: effect on reaction kinetics, gel characteristics, physical and mechanical properties. RSC Adv 6(45):39106–39117
18. Andric L et al (2014) Comparative kinetic study of mechanical activation process of mica and talc for industrial application. Compos B Eng 59:181–190
19. Hrachova J et al (2007) Dry grinding of Ca and octadecyltrimethylammonium montmorillonite. J Colloid Interface Sci 316(2):589–595
20. Ilić B et al (2016) Effects of mechanical and thermal activation on pozzolanic activity of kaolin containing mica. Appl Clay Sci 123:173–181
21. Souri A et al (2015) Pozzolanic activity of mechanochemically and thermally activated kaolins in cement. Cem Concr Res 77:47–59
22. Vdović N et al (2010) The surface properties of clay minerals modified by intensive dry milling—revisited. Appl Clay Sci 48(4):575–580
23. Yao G et al (2019) Effect of mechanical activation on the pozzolanic activity of muscovite. Clays Clay Miner 67(3):209–216
24. Ke X, Baki VA, Skevi L (2023) Mechanochemical activation for improving the direct mineral carbonation efficiency and capacity of a timber biomass ash. J CO2 Utilizat. 68: 102367.
25. Ryou J (2004) Improvement on reactivity of cementitious waste materials by mechanochemical activation. Mater Lett 58(6):903–906
26. Skevi L et al (2022) Biomass bottom ash as supplementary cementitious material: the effect of mechanochemical pre-treatment and mineral carbonation. Materials 15(23):8357
27. BS EN 196-1 (2016) Methods of testing cement. Determination of strength. 2016, British Standards Institute
28. Dellisanti F, Valdre G (2005) Study of structural properties of ion treated and mechanically deformed commercial bentonite. Appl Clay Sci 28(1–4):233–244
29. Mitrovic A, Zdujic M (2014) Preparation of pozzolanic addition by mechanical treatment of kaolin clay. Int J Miner Process 132:59–66
30. Aglietti EF, Porto Lopez JM, Pereira E (1986) Mechanochemical effects in kaolinite grinding. II. Structural aspects. Int J Min Process 16(1–2):135–146
31. Aglietti EF, Porto Lopez JM, Pereira E (1986) Mechanochemical effects in kaolinite grinding. I. Textural and physicochemical aspects. Int J Miner Process. 16(1–2):125–133
32. Aglietti EF, Lopez JMP (1992) Physicochemical and Thermal-Properties of Mechanochemically Activated Talc. Mater Res Bull 27(10):1205–1216
33. Cordeiro GC et al (2011) Influence of particle size and specific surface area on the pozzolanic activity of residual rice husk ash. Cement Concr Compos 33(5):529–534
34. Shinohara AH et al (1993) Effects of moisture on grinding of natural calcite by a tumbling ball mill. Adv Powder Technol 4(4):311–319
35. Weerdt KD (2023) Separate grinding versus intergrinding Advanced cementing materials Reduced CO2—emissions 2007; Available from: https://www.sintef.no/globalassets/sintef-byggforsk/coin/sintef-reports/sbf-bk-a07022_separate-grinding-versus-intergrinding.pdf
36. Pérez A et al (2018) Influence Grinding Procedure, Limestone Content and PSD of Components on Properties of Clinker-Calcined Clay-Limestone Cements Produced by Intergrinding. In: Calcined Clays for Sustainable Concrete. Springer, Dordrecht
37. Kristóf É (1993) The effect of mechanical treatment on the crystal structure and thermal behavior of kaolinite. Clays Clay Miner 41(5):608–612
38. Cheng SK et al (2021) Pozzolanic activity of mechanochemically and thermally activated coal-series kaolin in cement-based materials. Constr Build Mater 299:123972
39. Frost RL et al (2001) Mechanochemical treatment of kaolinite. J Colloid Interface Sci 239(2):458–466
40. Andrini L et al (2017) Extended and local structural characterization of a natural and 800 degrees C fired Na-montmorillonite-Patagonian bentonite by XRD and Al/Si XANES. Appl Clay Sci 137:233–240
41. Fernandez R, Martirena F, Scrivener KL (2011) The origin of the pozzolanic activity of calcined clay minerals: a comparison between kaolinite, illite and montmorillonite. Cem Concr Res 41(1):113–122
42. Allegretta I, Pinto D, Eramo G (2016) Effects of grain size on the reactivity of limestone temper in a kaolinitic clay. Appl Clay Sci 126:223–234
43. Li TT et al (2014) Effects of dry grinding on the structure and granularity of calcite and its polymorphic transformation into aragonite. Powder Technol 254:338–343
44. Chen YR et al (2015) Effects of rotation speed and media density on particle size distribution and structure of ground calcium carbonate in a planetary ball mill. Adv Powder Technol 26(2):505–510
45. Dellisanti F et al (2018) Effects of dehydration and grinding on the mechanical shear behaviour of Ca-rich montmorillonite. Appl Clay Sci 152:239–248
46. Kalinkina EV et al (2001) Sorption of atmospheric carbon dioxide and structural changes of Ca and Mg silicate minerals during grinding—I. Diopside Int J Min Processng 61(4):273–288
47. Borouni M, Niroumand B, Maleki A (2018) A study on crystallization of amorphous nano silica particles by mechanical activation at the presence of pure aluminum. J Solid State Chem 263:208–215
48. Saikia NJ et al (2003) Characterization, beneficiation and utilization of a kaolinite clay from Assam. India Applied Clay Science 24(1–2):93–103
49. Srasra E, Bergaya F, Fripiat JJ (1994) Infrared-spectroscopy study of tetrahedral and octahedral substitutions in

an interstratified illite-smectite clay. Clays Clay Miner 42(3):237–241
50. Bell RJ, Hibbins-Butler DC (1976) Infrared activity of normal modes in vitreous silica, Germania and beryllium fluoride. J Phys C Solid State Phys 9(7):1171–1175
51. Gnisci A (2022) Preliminary characterization of hydraulic components of low-temperature calcined marls from the south of Italy. Cem Concr Res 161:106958
52. Karunadasa KSP et al (2019) Thermal decomposition of calcium carbonate (calcite polymorph) as examined by in-situ high-temperature X-ray powder diffraction. J Phys Chem Solids 134:21–28
53. Mako E et al (2001) The effect of quartz content on the mechanochemical activation of kaolinite. J Colloid Interface Sci 244(2):359–364
54. Guzzo PL, de Barros FBM, Tino AAD (2019) Effect of prolonged dry grinding on size distribution, crystal structure and thermal decomposition of ultrafine particles of dolostone. Powder Technol 342:141–148
55. Li XR et al (2018) Reactivity tests for supplementary cementitious materials: RILEM TC 267-TRM phase 1. Mater Struct 51(6):151
56. Ferone C et al (2015) Thermally treated clay sediments as geopolymer source material. Appl Clay Sci 107:195–204
57. Lothenbach B et al (2008) Influence of limestone on the hydration of Portland cements. Cem Concr Res 38(6):848–860
58. Plusquellec G et al. (2021) Activated Swedish clays as supplementary cementitious material
59. De Weerdt K et al (2011) Hydration mechanisms of ternary Portland cements containing limestone powder and fly ash. Cem Concr Res 41(3):279–291
60. International A (2012) ASTM C618, Standard Specification for Coal Ash and Raw or Calcined Natural Pozzolan for Use in Concrete. 2014: West Conshohocken, PA, USA
61. Benezet JC, Benhassaine A (2009) Contribution of different granulometric populations to powder reactivity. Particuology 7(1):39–44